*Cancer Imaging* (2012) **12,** 72–78
DOI: 10.1102/1470-7330.2012.0009

CI

e-med
www.e-med.org.uk

ORIGINAL ARTICLE

# Gadoxetate acid-enhanced MRI of hepatocellular carcinoma in a c-myc/TGF$\alpha$ transgenic mouse model including signal intensity and fat content: initial experience

**Huedayi Korkusuz[a], Lea Knau[b], Wolfgang Kromen[b], Frank Huebner[b], Renate Hammerstingl[b], Sebastian Lindemayr[b], Verena Bihrer[c], Albrecht Piiper[c], Thomas J Vogl[b]**

*[a]Department of Nuclear Medicine, Johann Wolfgang Goethe University Hospital, Theodor-Stern-Kai 7, D-60590 Frankfurt, Germany; [b]Department of Diagnostic and Interventional Radiology, Johann Wolfgang Goethe University Hospital, Theodor-Stern-Kai 7, D-60590 Frankfurt, Germany; [c]Department of Medicine I, Johann Wolfgang Goethe University Frankfurt, Theodor-Stern-Kai 7, 60590 Frankfurt, Germany*

*Corresponding address: Huedayi Korkusuz, Department of Nuclear Medicine, Johann Wolfgang Goethe University, Theodor-Stern-Kai 7, 60590 Frankfurt, Germany.*
*Email:* huedayi.korkusuz@kgu.de

Date accepted for publication 9 December 2011

**Abstract**

Genetically engineered mouse models, such as double transgenic c-myc/TGF$\alpha$ mice, with specific pathway abnormalities might be more successful at predicting the clinical response of hepatocellular carcinoma (HCC) treatment. But a major drawback of the tumour models is the difficulty of visualizing endogenously formed tumours. The optimal imaging procedure should be brief and minimally invasive. Magnetic resonance imaging (MRI) satisfies these criteria and gadoxetate acid-enhanced MRI improves the detection of HCC. Fat content is stated to be an additional tool to help assess tumour responses, for example, in cases of radiofrequency ablation. Therefore the aim of this study was to investigate if gadoxetate acid-enhanced MRI could be used to detect HCC in c-myc/TGF$\alpha$ transgenic mice by determining the relation between the signal intensity of HCC and normal liver parenchyma and the corresponding fat content as a diagnostic marker of HCC. In our study, 20 HCC in c-myc/TGF$\alpha$ transgenic male mice aged 20–34 weeks were analyzed. On gadoxetate acid-enhanced MRI, the signal intensity was 752.4 for liver parenchyma and 924.5 for HCC. The contrast to noise ratio was 20.4, the percentage enhancement was 267.1% for normal liver parenchyma and 353.9% for HCC. The fat content was 11.2% for liver parenchyma and 16.2% for HCC. There was a correlation between fat content and signal intensity with $r = 0.7791$. All parameters were statistically significant with $P < 0.05$. Our data indicate that gadoxetate acid contrast enhancement allows sensitive detection of HCC in c-myc/TGF$\alpha$ transgenic mice and determination of the fat content seems to be an additional useful parameter for HCC.

**Keywords:** *MRI; hepatocellular carcinoma; gadoxetate acid; c-myc/TGF$\alpha$ transgenic mouse model; fat content.*

## Introduction

Hepatocellular carcinoma (HCC) is a malignant disease of the liver and one of the most common malignancies worldwide[1]. HCC, has a poor prognosis and develops based on steatohepatitic and cirrhotic predamaged liver parenchyma. The poor prognosis of HCC is a consequence of the detection of HCC at advanced stages, at which curative options such as transplantation, surgical resection or local ablation are not available. Therefore in the last few years new approaches were developed to improve early detection of HCC and to improve

This paper is available online at http://www.cancerimaging.org. In the event of a change in the URL address, please use the DOI provided to locate the paper.

 © 2012 International Cancer Imaging Society

monitoring therapeutic success. Appropriately designed mouse models would be highly useful to facilitate the development of new tumour diagnostics and therapies. However, neither cell-based assays nor xenograft models are particularly successful in predicting drug responses in humans. Genetically engineered mouse models recapitulating specific pathway abnormalities such as double transgenic c-myc/TGF$\alpha$ mice might be more successful at predicting clinical response[2,3]. A major drawback of the tumour models is the difficulty to visualize the endogenously formed tumours. Optimal imaging procedure should be brief and minimally invasive[3]. Magnetic resonance imaging (MRI) satisfies these criteria and gadoxetate acid (Primovist, Bayer Schering Pharma AG, Berlin, Germany)-enhanced MRI improves the detection of HCC[4,5] and has a better performance than computed tomography or unenhanced MRI[6] and MDCT[7] in humans.

Gadoxetate acid (gadolinium ethoxybenzyl diethylenetriamine pentaacetic acid) is a liver-specific lipophilic contrast agent, behaving both as an extracellular and hepatobiliary agent[8]. Most malignant lesions including HCCs and metastatic liver tumours do not take up gadoxetate acid, resulting in detection of tumours as hypointense nodules on the hepatobiliary phase of gadoxetate acid-enhanced MRI. Accordingly, 92% of human HCCs appear as hypointense nodules in gadoxetate acid-enhanced MRI, but 3% show a hyperintense signal due to the overexpression of a particular sodium independent organic anion transporter[9]. Changes in the fatty component are one prognostic marker. Fat content is stated to be an additional tool to help assess tumour responses and to determine treatment success or failure of radiofrequency ablation[10]. To verify a correlation between the signal intensity of gadoxetate acid-enhanced MRI and the fat content of HCC, the fat content of HCC was specified by Dixon in-phase (IP) and opposed-phase (OP) MRI, confirmed by histopathologic analysis and compared with the signal intensity of gadoxetate acid-enhanced T1 weighted fat-suppressed MRI.

The aim of this study was to evaluate gadoxetate acid-enhanced MRI in a c-myc/TGF$\alpha$ transgenic mouse model for detecting HCC by determining the relationship between the signal intensity and the fat content of HCC.

## Materials and methods

### *Animals*

Twenty-one c-myc/TGF$\alpha$ transgenic mice aged 20–34 weeks were examined by gadoxetate acid-enhanced MRI. These double transgenic male c-myc/TGF$\alpha$ mice were generated by breeding the homozygous single transgenic mice. Hepatocarcinogenesis was induced by zinc in the drinking water, resulting in 100% incidence of HCC after 6–9 months[11,12]. These animals show an overexpression of the oncogene c-myc and of transforming growth factor-alpha (TGF-$\alpha$). The process was confirmed by pathologic examination after MRI analysis. The c-myc/TGF$\alpha$ transgenic mouse model was established by Thorgeirsson et al. (National Cancer Institute, NIH, Bethesda, MD, USA) to investigate the molecular events underlying human hepatic malignant transformation. The governmental committee and our institutional animal research review board approved this study.

### *MRI method*

MRI was performed by 3-T MRI (Siemens Magnetom Trio, Erlangen, Germany). An MRI coil for 3-T (8 channel multifunctional coil; NORAS MRI Products GmbH, Höchberg, Germany) was used to increase the signal. Each coil was configured as a 4-channel array. All images were obtained in the axial plane. The imaging sequences included T1-weighted turbo-spin echo with the following parameters: echo time (TE) = 20 ms, repetition time (TR) = 947 ms, field of view = 100 mm, slice thickness = 1 mm, flip angle = 140° and fat suppression = fat saturation. The imaging sequences for determination of fat content were: IP: TR = 5.96 ms, TE = 2.45 ms, slice thickness = 1 mm; OP: TR = 5.96 ms, TE = 3.675 ms, slice thickness = 1 mm. The spatial resolution (matrix) was $160 \times 160$ with a voxel size of $1.2 \times 1.2 \times 1$ mm.

Mice were anesthetized by intraperitoneal administration of ketamine and xylazine. Then 200 µl of 10 mM gadoxetate acid were injected into the retrobulbar venous plexus before MRI. The imaging sequences for determination of fat content were performed immediately after administration of contrast agent. The sequences to determine the signal intensity of liver parenchyma and HCC were obtained before and 20 min after administration of contrast medium.

### *Image analysis*

All MRI examinations were transferred to a picture archiving and communication system (PACS; Centricity, Chicago, IL, USA) viewing station. Each lesion was evaluated by statistical analysis based on the measurement of the signal intensity of T1-weighted MRI by operator-defined regions of interest (ROI). The signal intensity of liver and HCC were determined. Five ROIs were selected in normal liver parenchyma, avoiding blood vessels, and 5 ROIs were selected in HCC. The contrast to noise ratio and percentage enhancement were calculated based on these values (Table 1). They were expressed as means ± standard deviation (SD).

### *Statistical analysis*

To assess one normally distributed, independent sample, the one-sample *t* test was used. In the case of 2 non-normally distributed independent samples, the non-parametric Mann-Whitney test was used. Results were considered to be significant at $P < 0.05$. Linear regression

***Table 1*** **Calculation of the statistical parameters of gadoxetate acid-enhanced MRI**

| Parameter | Formula | Unit |
|---|---|---|
| Contrast to noise ratio | (Signal intensity of HCC − signal intensity of liver parenchyma)/SD image noise | – |
| Percentage enhancement | [(Signal intensity of Gd-EOB-DTPA-enhanced − signal intensity of unenhanced)/signal intensity if unenhanced] × 100 | % |

Formulas to calculate the contrast to noise ratio and percentage enhancement for image analysis of gadoxetate acid-enhanced MRI of c-myc/TGF$\alpha$ transgenic mice using the signal intensity and standard deviation (SD) of normal liver parenchyma and HCC.

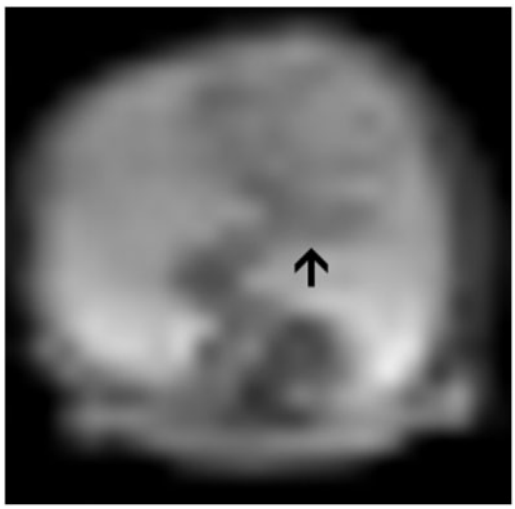

***Figure 1*** **Gadoxetate acid-enhanced MRI of a c-myc/ TGF$\alpha$ mouse. IP chemical shift MR images of the same lesion (arrow) as in Fig. 3.**

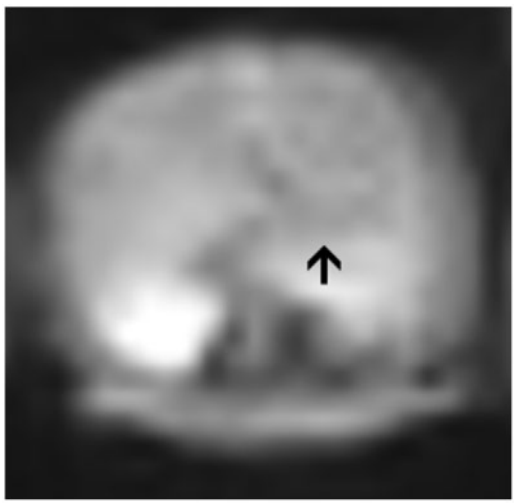

***Figure 2*** **Gadoxetate acid-enhanced MRI of a c-myc/ TGF$\alpha$ mouse. OP chemical shift MR images of the same lesion (arrow) as in Fig. 3.**

was determined by single linear regression (Pearson) and the analysis of matched pairs was performed using the Wilcoxon matched pairs test.

### *Determination of fat content*

Fat content in MRI was calculated using a formula in Dixon T1 IP and OP MRI sequences, as shown in Figs. 1 and 2[13]. Five ROIs on each gadoxetate acid-enhanced image were selected on IP and OP sequences in normal liver tissue as well as in HCC. They were expressed as means ± SD. The fat content was estimated applying the following formulas:

$$\text{Fat content liver} = \frac{(\text{liver signal intensity IP} - \text{liver signal intensity OP})}{\text{liver signal intensity IP}} \times 100$$

$$\text{Fat content HCC} = \frac{(\text{HCC signal intensity IP} - \text{HCC signal intensity OP})}{\text{HCC signal intensity IP}} \times 100$$

### *Histologic analysis*

The resected liver specimens were fixed in 4% formalin and cut in their entirety in 3-mm slices to facilitate careful gross examination. Specimens were embedded in paraffin, cut in 4-μm sections, and stained with hematoxylin and eosin for histopathologic evaluation.

## Results

Twenty-one c-myc/TGF$\alpha$ transgenic mice with HCC were used to detect HCC by gadoxetate acid-enhanced MRI. One mouse was excluded from this study because T1 IP and OP images could not be analyzed for the determination of fat content.

### *Gadoxetate acid-enhanced MRI parameters*

T1-weighted MRI of the liver in a c-myc/ TGF$\alpha$ mouse with HCC is shown in Fig. 3. On gadoxetate acid administration, 20 HCC appeared hyperintense in T1-weighted fat-suppressed MRI. The signal intensity is statistically significantly different compared with unenhanced images and the comparison between the signal intensity of the liver and HCC was statistically significant ($P < 0.05$) (Table 2).

The difference between the signal intensity of the tumour and the liver parenchyma in relation to the background noise was $20.4 \pm 8.3$ ($P < 0.05$).

The percentage enhancement of unenhanced compared with gadoxetate acid-enhanced liver parenchyma was $267.1 \pm 30.6\%$ and $353.9 \pm 39.1$ for HCC (Table 2). This comparison was statistically significant ($P < 0.05$). The comparison between the percentage enhancement values of HCC and liver parenchyma revealed that gadoxetate acid enhancement of HCC was $84.3 \pm 35.4\%$ higher than that of normal liver parenchyma.

### *Correlation of fat content and signal intensity*

All mice had steatosis and fatty HCC. The mean value of the fat content based on McPherson's formula was $11.2 \pm 1.5\%$ for liver parenchyma and $16.2 \pm 2.7\%$ for HCC. According to these values, the difference between the fat content in liver parenchyma and HCC was statistically significant with $P < 0.05$ (Table 2). There was a correlation between fat content and signal intensity of $r = 0.7791$ (Pearson) as shown in Fig. 4. The comparison of these matched pairs was statistically significant ($P < 0.05$).

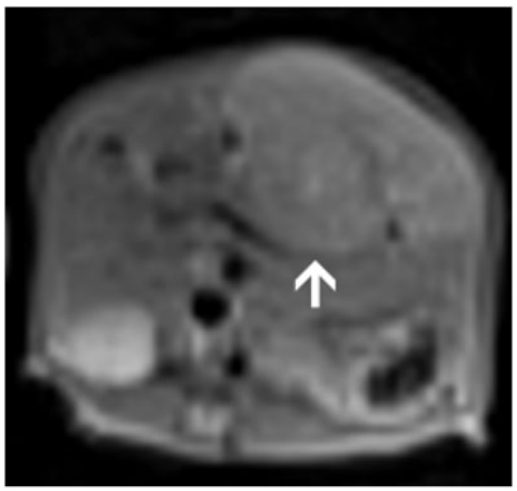

***Figure 3*** **Gadoxetate acid-enhanced MRI of a c-myc/TGF$\alpha$ mouse. T1-weighted 3-T MRI with HCC (arrow) with hyperintensive enhancement.**

The pathologic diagnosis and evaluation of the fat content was made based on resected livers post mortem. Histologic patterns were primarily well-differentiated HCCs with a Dixon score of 2 and a fat content of 5–25%, representing mild fatty degeneration (Fig. 5).

## Discussion

Previous studies have shown that MRI is highly useful for the diagnosis of hepatic lesions. In particular, gadoxetate acid considerably improved the detection of HCC[14–18]. Other studies have shown that T1-weighted fat-suppressed images are superior to other imaging techniques such as non-fat-suppressed T1-weighted or T2-weighted images[19].

The results of this study confirm that gadoxetate acid is useful to detect HCC in the c-myc/TGF$\alpha$ transgenic mouse model. This is shown by the signal intensity, contrast to noise ratio and percentage enhancement. HCCs could be easily distinguished from normal liver parenchyma as demonstrated by the statistically significant difference in the signal intensity of normal liver

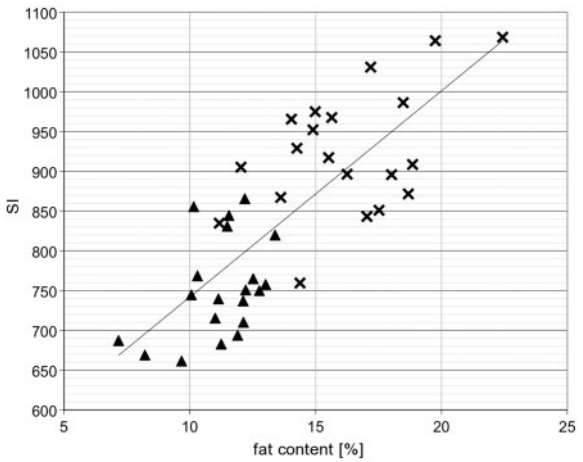


***Figure 4*** **Correlation of fat content and signal intensity of gadoxetate acid-enhanced liver parenchyma (triangle) and gadoxetate acid-enhanced HCC (cross) with $r = 0.7791$ (Pearson). The comparison of these matched pairs was statistically significant ($P < 0.05$) (Wilcoxon matched pairs test).**

***Table 2*** **Statistical parameters of gadoxetate acid-enhanced MRI**

| | HCC | Liver parenchyma | Mean difference: normal liver vs HCC | *P* value |
|---|---|---|---|---|
| Signal intensity | $924.5 \pm 78.7$ | $752.4 \pm 62.6$ | $172.03 \pm 24.4$ | <0.05* |
| Contrast to noise ratio | $20.4 \pm 8.3$ | | – | <0.05** |
| Percentage enhancement | $353.9 \pm 39.1$ | $267.1 \pm 30.6$ | $84.3 \pm 35.4$ | <0.05* |
| Fat content (%) | $16.2 \pm 2.7$ | $11.2 \pm 1.5$ | $5.02 \pm 3.03$ | <0.05*** |

*Wilcoxon-Mann-Whitney test.
**One-sample *t* test.
***Wilcoxon matched pairs test.

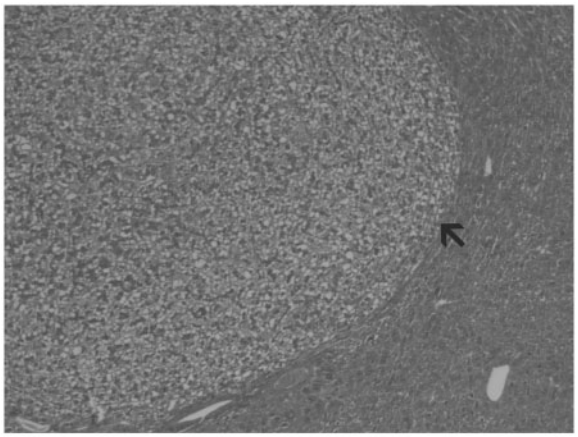

***Figure 5*** **Normal liver parenchyma and liver tumour (arrow) with a Dixon score of 2.**

parenchyma compared with HCCs. Even more important for the evaluation of the relation between normal liver parenchyma and HCC of gadoxetate acid enhancement is the contrast to noise ratio, which confirmed the difference in signal intensity between HCC and liver parenchyma and excluded the influence of the image noise.

Percentage enhancement also verified the benefit of gadoxetate acid-enhanced MRI in that HCCs showed an increased uptake of gadoxetate acid compared with normal liver parenchyma by $84.3 \pm 35.4\%$. In addition, fatty HCCs are associated with a high signal intensity. This reflects that HCCs contain a higher fat content than liver parenchyma. This was confirmed by histology and a higher signal intensity than the surrounding normal liver parenchyma. On the other hand, normal liver tissue has a low fat content and according to this, a low signal intensity. In conclusion, a high percentage enhancement is associated by a high fat content.

## *Reason for hyperintensive gadoxetate acid enhancement: hepatic gadoxetate acid uptake*

Other studies addressing the reason for gadoxetate acid enhancement of HCC in MRI stated that the grade of cell differentiation[20,21], bile production[16], or necrosis of HCC[22] did not correlate with the enhancement ratio of gadoxetate acid. The enhancement ratios correlate with lesion size[23], bile accumulation in tumours[24] and with levels of sodium independent organic anion transporters, because hepatocellular uptake of gadoxetate acid is considered to represent passive diffusion mediated by organic anion transporter polypeptide 1 (OATP1), which is expressed on the hepatocyte membrane. According to this hypothesis, HCC appear hyperintensive in gadoxetate acid-enhanced MRI because of the overexpression of transporters such as OATP1B1, OATP1B3 and NTCP[24–27].

## *Gadoxetate acid characteristics in hepatocytes*

After the uptake of gadoxetate acid, the lipophilic contrast agent remains in the hepatocytes. Our study shows a correlation between gadoxetate acid-enhanced signal intensity and fat content ($r = 0.7791$), which is visualized in Fig. 4. HCCs often contain an adipose component and show various grades of fatty infiltration, which may be diffuse throughout the tumour, in focal areas or in a patchy pattern. The fat content was even more frequent in small HCC nodules[10,28]. The mean value of fat content was 16.2% for HCCs and 11.2% for normal liver parenchyma in c-myc/TGF$\alpha$ mice. This suggests that the metabolic activity is reprogrammed towards steatosis. This internal fat deposition is assessed by quantification of intrahepatocellular lipid by MRI by exploiting characteristic differences in resonant frequencies between protons in fat and water environments, determining the differences in intensity between IP and OP images[29–31]. MRI is proven to be comparably accurate in quantifying hepatic fat content[32] and neither interaction between Dixon IP/OP or $\pm$ fat saturation and stage of fibrosis or hepatic inflammation affect the accuracy of MRI for the assessment of steatosis[29]. Therefore, MRI is an elegant method for the non-invasive quantification of the hepatic fat content[32].

Increased lysophosphatidic acid (LPA) may provide a potent mitogenic and proliferative microenvironment via autocrine and paracrine activation of high-affinity G-protein-coupled receptors and cellular proliferation is accompanied by reprogramming of metabolic activity, such as high rates of glycolysis, lactate production and lipid biosynthesis. Hence lipids are linked to pathologic process such as inflammation, obesity and liver disease, and they are involved in cellular signaling[33]. They are also involved in apoptosis and cell cycle regulation[34]. Specific receptors, Rho and Rho kinase, have the ability to stimulate cell proliferation. For that reason, LPA signaling has been linked to cancer, which means that an overexpression of Rho-GTPase binding proteins is associated with lysophosphatidic acid signaling. The current hypothesis is that control of metabolic activity in tumour cells is synchronous with that of growth factor signaling. The fat content in HCC and in liver parenchyma of c-myc/TGF$\alpha$ transgenic mice make it likely that growth factor signaling regulates metabolic activity[33]. This may explain the high fat content of HCC compared with normal liver parenchyma. Thus, the increased fat content of HCC may retain gadoxetate acid in HCC cells, preventing hepatic secretion via the multidrug-resistance associated proteins, ABCB4 and ABCC2[26].

## *Fat content as a prognostic marker of successful therapy*

Fat content is a valuable predictor of successful therapy. This is demonstrated by other studies. They stated that

visceral fat accumulation, which is related to the severity of fatty liver, increases the risk of HCC development and is an independent risk factor of HCC after curative treatment[35]. In particular, a high fat content of the liver, with regard to non-alcoholic steatohepatitis, is a risk factor for HCC[36–38]. Other risk factors are age >62 years, poor histopathologic grading, multifocal tumour, portal vein thrombosis, higher alpha-fetoprotein and serum bilirubin levels[38,39]. The risk factor fat content can be surveyed by gadoxetate acid-enhanced MRI. In accordance with our results that fat content and signal intensity correlate, high signal intensity by gadoxetate acid-enhanced MRI might be used as a prognostic marker of successful therapy. According to this, changes in the fatty component might be used to monitor therapy. Thus, Pupulim et al.[10] demonstrated monitoring for therapy success of radiofrequency ablation.

### *Benefit of gadoxetate acid-enhanced MRI in the c-myc/TGFα mouse model*

Transgenic HCC mouse models such as the c-myc/TGFα model used in the present study are valuable for detecting HCC due to its similarity to human HCC. The advantage of mouse models in research has already been shown by the detection of HCC initiation and progression in transgenic mouse models such as alb-myctg with clinical 1.5-T MR scanners and gadoxetate acid enhancement by revealing hypointense lesions[40].

The second advantage of gadoxetate acid-enhanced MRI for detecting HCC is the relation between signal intensity and fat content. Our study indicates that one reason for gadoxetate acid enhancement is steatosis. Therefore, changes in the fatty component could be an additional finding to help to assess tumour responses and success of therapy. This was revealed by a study of radiofrequency ablation of fatty HCCs and suggests that fat content could be used as a prognostic marker for HCC therapy[10].

### *Limitations*

Even though this transgenic mouse model for detecting HCC has many advantages, such as histologic similarity to human tumours, the tumours arise in immunocompetent mice, metastatic distribution similar to the clinical situation, relevant host immune cell infiltration and tumour microenvironment[40], the results of gadoxetate acid enhancement cannot uncritically be transferred to humans.

## Conclusion

Highly hepatocyte-selective enhancement of gadoxetate acid is correlated with the amount of HCC fat content. Gadoxetate acid enhancement, based on its correlation with the fat content, might be a useful tool as a prognostic marker or for monitoring therapy. This animal model may help to develop a better understanding of HCC gadoxetate acid contrast enhancement and thus of HCC diagnostics and therapy.

## Acknowledgement

We thank Snorri S. Thorgeirsson (National Cancer Institute, NIH, Bethesda, MD, USA) for kindly providing c-myc/TGFα transgenic mice.

## References

[1] Kudo M. Multistep human hepatocarcinogenesis: correlation of imaging with pathology. J Gastroenterol 2009; 44(Suppl 19): 112–18. doi:10.1007/s00535-008-2274-6.

[2] Newell P, Villanueva A, Llovet JM. Molecular targeted therapies in hepatocellular carcinoma: from pre-clinical models to clinical trials. J Hepatol 2008; 49: 1–5. doi:10.1016/j.jhep.2008.04.006.

[3] Olive KP, Tuveson DA. The use of targeted mouse models for preclinical testing of novel cancer therapeutics. Clin Cancer Res. 2006; 12: 5277–87. doi:10.1158/1078-0432.CCR-06-0436.

[4] Kanematsu M, Kondo H, Goshima S, Tsuge Y, Watanabe H. Magnetic resonance imaging of hepatocellular carcinoma. Oncology 2008; 75(Suppl 1): 65–71. doi:10.1159/000173426.

[5] Montfoort JEV, Stieger B, Meijer DK, Weinmann HJ, Meier PJ, Fattinger KE. Hepatic uptake of the magnetic resonance imaging contrast agent gadoxetate by the organic anion transporting polypeptide Oatp1. J Pharmacol Exp Ther 1999; 290: 153–7.

[6] Ichikawa T, Saito K, Yoshioka N, et al. Detection and characterization of focal liver lesions: a Japanese Phase III, multicenter comparison between gadoxetic acid disodium-enhanced magnetic resonance imaging and contrast-enhanced computed tomography predominantly in patients with hepatocellular carcinoma and chronic liver disease. Invest Radiol 2010; 45: 133–41. doi:10.1097/RLI.0b013e3181caea5b.

[7] Kim YK, Kim CS, Han YM, et al. Detection of hepatocellular carcinoma: gadoxetic acid-enhanced 3-dimensional magnetic resonance imaging versus multi-detector row computed tomography. J Computer Assist Tomogr 2009; 33: 844–50. doi:10.1097/RCT.0b013e3181a7e3c7.

[8] Vogl TJ, Kümmel S, Hammerstingl R, et al. Liver tumors: comparison of MR imaging with Gd-EOB-DTPA and Gd-DTPA. Radiology 1996; 200: 59–67.

[9] Kogita S, Imai Y, Okada M, et al. Gd-EOB-DTPA-enhanced magnetic resonance images of hepatocellular carcinoma: correlation with histological grading and portal blood flow. Eur Radiol 2010; 20: 2405–13. doi:10.1007/s00330-010-1812-9.

[10] Pupulim LF, Hakimé A, Barrau V, Abdel-Rehim M, Zappa M, Vilgrain V. Fatty hepatocellular carcinoma: radiofrequency ablation: imaging findings. Radiology 2009; 250: 940–8. doi:10.1148/radiol.2502080858.

[11] Calvisi DF, Thorgeirsson SS. Molecular mechanisms of hepatocarcinogenesis in transgenic mouse models of liver cancer. Toxicol Pathol 2005; 33: 181–4. doi:10.1080/01926230590522095.

[12] Murakami H, Sanderson ND, Nagy P, Marino PA, Merlino G, Thorgeirsson SS. Transgenic mouse model for synergistic effects of nuclear oncogenes and growth factors in tumorigenesis: interaction of c-myc and transforming growth factor alpha in hepatic oncogenesis. Cancer Res 1993; 53: 1719–23.

[13] McPherson S, Jonsson JR, Cowin GJ, et al. Magnetic resonance imaging and spectroscopy accurately estimate the severity of steatosis provided the stage of fibrosis is considered. J Hepatol 2009; 51: 389–97. doi:10.1016/j.jhep.2009.04.012.

[14] Ahn SS, Kim M, Lim JS, Hong HS, Chung YE, Choi JY. Added value of gadoxetic acid-enhanced hepatobiliary phase MR

imaging in the diagnosis of hepatocellular carcinoma. Radiology 2010; 255: 459–66. doi:10.1148/radiol.10091388.

[15] Shimofusa R, Ueda T, Kishimoto T, et al. Magnetic resonance imaging of hepatocellular carcinoma: a pictorial review of novel insights into pathophysiological features revealed by magnetic resonance imaging. J Hepato-Biliary-Pancreatic Surg 2009; 17: 583–9. doi:10.1007/s00534-009-0198-z.

[16] Reimer P, Rummeny EJ, Daldrup HE, et al. Enhancement characteristics of liver metastases, hepatocellular carcinomas, and hemangiomas with Gd-EOB-DTPA: preliminary results with dynamic MR imaging. Eur Radiol 1997; 7: 275–80. doi:10.1007/s003300050150.

[17] Tanimoto A, Lee JM, Murakami T, Huppertz A, Kudo M, Grazioli L. Consensus report of the 2nd International Forum for Liver MRI. Eur Radiol 2009; 19(Suppl 5): S975–89. doi:10.1007/s00330-009-1624-y.

[18] Motosugi U, Ichikawa T, Sou H, et al. Liver parenchymal enhancement of hepatocyte-phase images in Gd-EOB-DTPA-enhanced MR imaging: which biological markers of the liver function affect the enhancement? J Magn Reson Imaging 2009; 30: 1042–6. doi:10.1002/jmri.21956.

[19] Koushima Y, Ebara M, Fukuda H, et al. Small hepatocellular carcinoma: assessment with T1-weighted spin-echo magnetic resonance imaging with and without fat suppression. Eur J Radiol 2002; 41: 34–41. doi:10.1016/S0720-048X(01)00346-1.

[20] Frericks BB, Loddenkemper C, Huppertz A, et al. Qualitative and quantitative evaluation of hepatocellular carcinoma and cirrhotic liver enhancement using Gd-EOB-DTPA. AJR Am J Roentgenol 2009; 193: 1053–60. doi:10.2214/AJR.08.1946.

[21] Fujita M, Yamamoto R, Takahashi M, et al. Paradoxic uptake of Gd-EOB-DTPA by hepatocellular carcinoma in mice: quantitative image analysis. J Magn Reson Imaging 1997; 7: 768–70. doi:10.1002/jmri.1880070426.

[22] Vossen JA, Buijs M, Geschwind JH, et al. Diffusion-weighted and Gd-EOB-DTPA-contrast-enhanced magnetic resonance imaging for characterization of tumor necrosis in an animal model. J Computer Assist Tomogr 2009; 33: 626–30. doi:10.1097/RCT.0b013e3181953df3.

[23] Bos ICVD, Hussain SM, Dwarkasing RS, et al. MR imaging of hepatocellular carcinoma: relationship between lesion size and imaging findings, including signal intensity and dynamic enhancement patterns. J Magn Reson Imaging 2007; 26: 1548–55.

[24] Tsuboyama T, Onishi H, Kim T, et al. Hepatocellular carcinoma: hepatocyte-selective enhancement at gadoxetic acid-enhanced MR imaging–correlation with expression of sinusoidal and canalicular transporters and bile accumulation. Radiology 2010; 255: 824–33. doi:10.1148/radiol.10091557.

[25] Narita M, Hatano E, Arizono S, et al. Expression of OATP1B3 determines uptake of Gd-EOB-DTPA in hepatocellular carcinoma. J Gastroenterol 2009; 44: 793–8. doi:10.1007/s00535-009-0056-4.

[26] Leonhardt M, Keiser M, Oswald S, et al. Hepatic uptake of the magnetic resonance imaging contrast agent Gd-EOB-DTPA, role of human organic anion transporters. Drug Metab Dispos 2010; 38: 1024–8. doi:10.1124/dmd.110.032862.

[27] Kudo M. Will Gd-EOB-MRI change the diagnostic algorithm in hepatocellular carcinoma? Oncology 2010; 78(Suppl 1): 87–93. doi:10.1159/000315235.

[28] Saito K, Kotake F, Ito N, et al. Gd-EOB-DTPA enhanced MRI for hepatocellular carcinoma: quantitative evaluation of tumor enhancement in hepatobiliary phase. Magn Reson Med Sci 2005; 4: 1–9. doi:10.2463/mrms.4.1.

[29] Dixon WT. Simple proton spectroscopic imaging. Radiology 1984; 153: 189–94.

[30] Hussain HK, Chenevert TL, Londy FJ, et al. Hepatic fat fraction: MR imaging for quantitative measurement and display–early experience. Radiology 2005; 237: 1048–55. doi:10.1148/radiol.2373041639.

[31] Schuchmann S, Weigel C, Albrecht L, et al. Non-invasive quantification of hepatic fat fraction by fast 1.0, 1.5 and 3.0 T MR imaging. Eur J Radiol 2007; 62: 416–22. doi:10.1016/j.ejrad.2006.12.009.

[32] Skill NJ, Scott RE, Wu J, Maluccio MA. Hepatocellular carcinoma associated lipid metabolism reprogramming. J Surg Res 20091–6.

[33] Griffitts J, Tesiram Y, Reid GE, Saunders D, Floyd RA, Towner RA. In vivo MRS assessment of altered fatty acyl unsaturation in liver tumor formation of a TGF alpha/c-myc transgenic mouse model. J Lipid Res 2009; 50: 611–622. doi:10.1194/jlr.M800265-JLR200.

[34] Ohki T, Tateishi R, Shiina S, et al. Visceral fat accumulation is an independent risk factor for hepatocellular carcinoma recurrence after curative treatment in patients with suspected NASH. Gut 2009; 58: 839–44. doi:10.1136/gut.2008.164053.

[35] Takuma Y, Nouso K. Nonalcoholic steatohepatitis-associated hepatocellular carcinoma: our case series and literature review. World J Gastroenterol 2010; 16: 1436–41. doi:10.3748/wjg.v16.i12.1436.

[36] Kawada N, Imanaka K, Kawaguchi T, et al. Hepatocellular carcinoma arising from non-cirrhotic nonalcoholic steatohepatitis. J Gastroenterol 2009; 44: 1190–4. doi:10.1007/s00535-009-0112-0.

[37] Hashizume H, Sato K, Takagi H, et al. Primary liver cancers with nonalcoholic steatohepatitis. Eur J Gastroenterol Hepatol 2007; 19: 827–34. doi:10.1097/MEG.0b013e3282748ef2.

[38] Kirchner G, Kirovski G, Hebestreit A, et al. Epidemiology and survival of patients with hepatocellular carcinoma in Southern Germany. Int J Clin Exp Med 2010; 3: 169–79.

[39] Freimuth J, Gassler N, Moro N, et al. Application of magnetic resonance imaging in transgenic and chemical mouse models of hepatocellular carcinoma. Mol Cancer 2010; 9: 94. doi:10.1186/1476-4598-9-94.

[40] Wu L, Tang Z, Li Y. Experimental models of hepatocellular carcinoma: developments and evolution. J Cancer Res Clin Oncol 2009; 135: 969–81. doi:10.1007/s00432-009-0591-7.